

## Ultrafast carrier dynamics in tetrahedral amorphous carbon: carrier trapping versus electron–hole recombination

E Carpene<sup>1,3</sup>, E Mancini<sup>1</sup>, C Dallera<sup>1</sup>, D Schwen<sup>2</sup>, C Ronning<sup>2</sup>  
and S De Silvestri<sup>1</sup>

<sup>1</sup> ULTRAS CNR-INFN, Dipartimento di Fisica, Politecnico di Milano,  
Piazza Leonardo da Vinci 32, 20133 Milano, Italy

<sup>2</sup> Zweites Physikalisches Institut, Universität Göttingen,  
Friedrich-Hund-Platz 1, 37077 Göttingen, Germany

E-mail: [ettore.carpene@fisi.polimi.it](mailto:ettore.carpene@fisi.polimi.it)

*New Journal of Physics* **11** (2007) 404

Received 31 July 2007

Published 8 November 2007

Online at <http://www.njp.org/>

doi:10.1088/1367-2630/9/11/404

**Abstract.** We report the investigation of the ultrafast carrier dynamics in thin tetrahedral amorphous carbon films by means of femtosecond time-resolved reflectivity. We estimated the electron–phonon relaxation time of a few hundred femtoseconds and we observed that under low optical excitation photo-generated carriers decay according to two distinct mechanisms attributed to trapping by defect states and direct electron–hole recombination. With high excitation, when photo-carrier and trap densities are comparable, a unique temporal evolution develops, as the time dependence of the trapping process becomes degenerate with the electron–hole recombination. This experimental evidence highlights the role of defects in the ultrafast electronic dynamics and is not specific to this particular form of carbon, but has general validity for amorphous and disordered semiconductors.

<sup>3</sup> Author to whom any correspondence should be addressed.

**Contents**

<b>1. Introduction</b>	<b>2</b>
<b>2. Experimental details</b>	<b>2</b>
<b>3. General formulation</b>	<b>3</b>
<b>4. Results and discussion</b>	<b>5</b>
<b>5. Conclusions</b>	<b>9</b>
<b>Acknowledgments</b>	<b>9</b>
<b>References</b>	<b>9</b>

**1. Introduction**

Hydrogen-free tetrahedral amorphous carbon (ta-C) has attracted much attention in the past decade due to its outstanding physical properties. Its diamond-like features emerge in the high mechanical hardness, chemical inertness, high thermal conductivity and large  $sp^3$  bonding fraction ( $>60\%$ ). Unlike diamond, it has a considerable potential as a semiconductor due to its p-type character and to the smaller optical gap (2–3 eV) [1]–[5]. From the electronic and structural viewpoints, the closest counterpart of ta-C is amorphous silicon (a-Si): recent studies in the sub-picosecond time domain have revealed that trapping by structural defects plays an important role in its ultrafast carrier dynamics [6]–[8]. It is well established that trapping centers in amorphous semiconductors are due to localized defect states originating from band tails reaching into the forbidden gap. These defects typically arise from incomplete or dangling bonds and deviation from the ideal  $sp^2$  or  $sp^3$  configurations [2, 9, 10]. The ability of ta-C to form a variety of chemical bonds ( $sp$ ,  $sp^2$  and  $sp^3$ ) is seen as a significant advantage compared to a-Si where hydrogen is generally used to passivate dangling bonds. Despite the large interest in ta-C, no investigation of its electronic properties on the femtosecond time scale has been undertaken to date. Time-resolved reflectivity measurements in the pump–probe configuration are particularly suitable for this purpose, since the dynamics of carriers photo-excited across the mobility gap can be studied by measuring the change in the reflectivity of the material. We have used this technique to investigate the ultrafast dynamics of injected carriers in a thin ta-C film. The transient reflectivity curves have been modeled, achieving excellent agreement with the experimental data. Besides, our analysis reveals that for low optical excitation, carrier trapping by defect states and electron–hole recombination determine the temporal decay of the carrier density. Increasing the optical pumping, if carrier and trap densities are comparable, electron–hole and trapping recombination mechanisms become indistinguishable. As it will be shown, this is an effect of the modified time dependence of the trapping process that has never been emphasized hitherto and provides an alternative interpretation of what has been invoked as *nonradiative* bimolecular recombination [6].

**2. Experimental details**

The ta-C film studied in this experiment was grown on n-type Si(111) substrate at room temperature by direct deposition of mass-separated  $^{12}C^+$  ions [11]. The energy of the carbon

ions was set to 100 eV, leading to an  $sp^3/sp^2$  ratio of about 80% [5]. Prior to the deposition, the substrate was sputter cleaned *in situ* using 1 keV  $Ar^+$  ions. The film is isotopically pure, hydrogen-free and about 150 nm thick. Time-resolved transient reflectivity has been measured with the standard pump–probe technique, using an amplified Ti:sapphire laser operating at a repetition rate of 1 kHz. Ultrashort pulses of 60 fs in duration, centered at 800 nm (1.55 eV) were used to probe the sample reflectivity. A portion of the amplified beam was employed to generate femtosecond pulses of the third harmonic, centered at 267 nm (4.65 eV) using  $\beta$ -BaB<sub>2</sub>O<sub>4</sub> (BBO) nonlinear optical crystals. We first generated second harmonic, centered at 400 nm (3.1 eV) through a BBO crystal. The residual infrared beam, rotated to the p-polarization state with a  $\lambda/2$  waveplate, was combined with the p-polarized second harmonic inside another BBO crystal, generating s-polarized third harmonic pulses with an estimated duration of 90 fs. The pump:probe spot size ratio was about 4 : 1. We have pumped the ta-C film with 4.65 eV photons, since the mobility gap of ta-C can be as large as 3 eV. In order to better understand the carrier dynamics, the pulse energy of the pump, focused on the sample to a spot size of about 500  $\mu$ m, was varied between 0.2 and 4  $\mu$ J.

### 3. General formulation

The relationship between free carriers and optical properties is based on the Drude model of the complex dielectric function  $\varepsilon(\omega)$ , an approach that is largely used and well documented in the literature [6, 12, 13]. In particular, when the energy of the probing photons is lower than the optical gap, the transient reflectivity  $\Delta R/R$  depends only on the variation  $\Delta n$  of real part of the complex refractive index  $\tilde{n} = n + ik$ , and in particular  $\Delta R/R = 4\Delta n/(n^2 - 1)$  [13, 14]. Considering that  $\Delta n$  can be explicitly made proportional to the carrier density  $N$  and to the lattice temperature rise  $\Delta T_L$ , i.e.  $\Delta n = N\partial n/\partial N + \Delta T_L\partial n/\partial T$ , the time dependence of the reflectivity reveals the temporal evolution of carrier density and lattice heating:

$$\frac{\Delta R}{R} = \frac{4}{n^2 - 1} \left( \frac{\partial n}{\partial N} N + \frac{\partial n}{\partial T} \Delta T_L \right). \quad (1)$$

The dependence of  $n$  on the carrier density  $N$  is calculated from the relationship between the dielectric function and the refractive index:  $\varepsilon(\omega) = \tilde{n}^2$ . In the limit  $(\omega\tau)^2 \gg 1$ <sup>4</sup> ( $\omega$  is the frequency of the probe electromagnetic wave and  $\tau$  is the carrier relaxation time appearing in the Drude expression of  $\varepsilon(\omega)$ ), the following relation can be obtained:

$$\frac{\partial n}{\partial N} = -\frac{1}{n} \left( \frac{q^2}{2\varepsilon_0 m \omega^2} \right) \quad (2)$$

with  $\varepsilon_0$  being the vacuum dielectric constant,  $m$  the carrier effective mass and  $q$  the electron charge. Using the electron mass  $m$  as the carrier effective mass [15], being  $\hbar\omega = 1.55$  eV and  $n \simeq 2.5$ <sup>5</sup>, we estimated  $\partial n/\partial N \simeq -1.1 \times 10^{-22}$  cm<sup>3</sup>. Considering that the ta-C film is about 150 nm thick and that the fluence of the probe beam is very low, the photo-induced bleaching due to the probe photons should be negligible. The thermo-optical coefficient  $\partial n/\partial T$  of

<sup>4</sup> This statement will be justified *a posteriori*.

<sup>5</sup> According to ellipsometry measurements on ta-C, at 1.5 eV photon energy,  $k \simeq 0.02$  and  $n \simeq 2.5$ , while at 4.5 eV,  $k \simeq 0.8$  and  $n \simeq 3$ . Accordingly, the optical absorption length for pump photons is about 30 nm, while for probe photons is about 3  $\mu$ m.

**Table 1.** Carrier recombination processes as determined by the solution of equation (3).  $N_m$  is the initial carrier density at  $t = 0$ ,  $\gamma_m$  is the characteristic recombination constant.

$m$	$N(t)$	Process
1	$N(t) = N_1 \exp(-\gamma_1 t)$	Trapping
2	$N(t) = N_2 / (1 + \gamma_2 N_2 t)$	Bimolecular
3	$N(t) = N_3 / \sqrt{1 + 2\gamma_3 N_3^2 t}$	Auger

ta-C is not known nor can it be reliably computed; however, as it will be shown, this will not significantly harm our analysis. Nonetheless, in analogy with similar investigations on a-Si [16, 17], we should expect a positive value of  $\partial n / \partial T$  also for ta-C.

Based on the vast literature about ultrafast carrier dynamics of a-Si, considered here as a benchmark for the electronic properties of amorphous semiconductors in the femtosecond time scale, the evolution of the carrier density following an optical excitation can be described by the general rate equation:

$$\frac{\partial N}{\partial t} = -\gamma_m N^m, \quad (3)$$

where  $\gamma_m > 0$  and  $1 \leq m \leq 3$  is an integer that identifies the possible recombination channels. The solutions of equation (3) are the analytical functions listed in table 1. If  $m = 1$ ,  $N$  decays exponentially with time constant  $\tau_1 = 1/\gamma_1$ . This process is attributed to carrier trapping, where  $\gamma_1 = N_t \sigma_t \langle v \rangle$  is proportional to the trap density  $N_t$ , the trap cross-section  $\sigma_t$  and the carrier thermal velocity  $\langle v \rangle$  [7, 8]. If  $m = 2$  ( $m = 3$ ), the carrier dynamics is due to electron–hole bimolecular recombination [6] (to three-body Auger-like process [12]), where  $\gamma_2$  ( $\gamma_3$ ) is the recombination constant. The Auger mechanism generally takes place with very strong excitation, when the photo-carrier density exceeds  $10^{20} \text{ cm}^{-3}$ , while electron–hole recombination and trapping should dominate the dynamics at moderate pumping [12, 14]. Lattice heating, on the other hand, is determined by the energy photo-excited carriers exchange with the lattice. Due to electron–phonon collisions, carriers lose energy emitting phonons, and the time evolution of the lattice temperature can be easily quantified: assuming  $U$  is the average energy of a photo-excited carrier and  $N$  is the carrier density, the rate of energy loss per unit volume (i.e. the energy transferred from carriers to the lattice) is  $N dU/dt \simeq NU/\tau_{ep}$ , with  $\tau_{ep}$  being the electron–phonon relaxation time. The increase of the lattice temperature  $T_L$  can be described by the relation:

$$c_p \frac{\partial T_L}{\partial t} = N \frac{dU}{dt} - c_p \frac{T_L}{\tau_{ep}} \simeq N \frac{U}{\tau_{ep}} - c_p \frac{T_L}{\tau_{ep}}, \quad (4)$$

where  $c_p$  is the lattice specific heat. Defining  $T_0 = NU/c_p$  leads to  $\partial T_L / \partial t = (T_0 - T_L) / \tau_{ep}$ , which can be easily solved, obtaining the time evolution of the lattice temperature:  $\Delta T_L = \Delta T_0 (1 - \exp(-t/\tau_{ep}))$ . Thus, the lattice temperature rises with a characteristic time constant  $\tau_{ep}$  that can be determined experimentally.

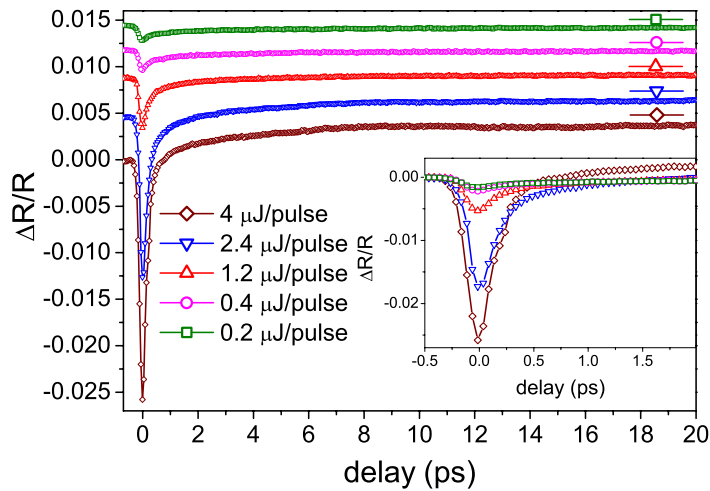


**Figure 1.** Time-resolved transient reflectivity of the ta-C film measured as a function of the pump–probe delay  $t$ . Different symbols (colors) correspond to different energies of the pump pulses (increasing energy from top to bottom). The curves have been offset for clarity. The inset shows in greater detail the delay region close to  $t = 0$  ps (without offset, increasing energy from top to bottom at  $t = 0$ ).

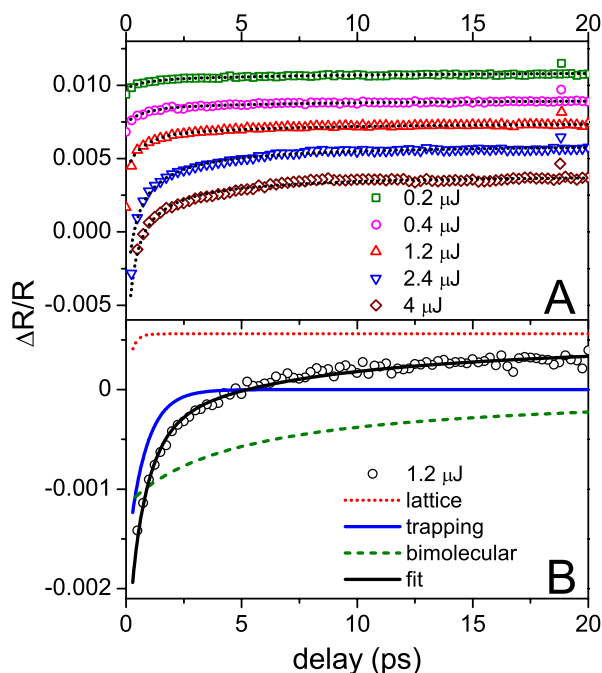
#### 4. Results and discussion

Figure 1 reports transient reflectivity  $\Delta R/R$  of the ta-C film measured as a function of the pump–probe delay, each scan corresponding to a different fluence of the pump. The rapid *negative* change around the delay  $t = 0$  ps (emphasized in the inset of figure 1) is determined by the ultrafast *increase* of the photo-excited carrier density  $N$  (in agreement with the negative sign of  $\partial n/\partial N$ , see equation (2)). At intermediate delays ( $0 < t < 1$  ps), the reflectivity recovers as a consequence of the carrier thermalization. However, for longer times ( $t > 2$  ps) and for high pump energies,  $\Delta R$  becomes *positive*, disclosing the effect of lattice heating and suggesting that the thermo-optical coefficient of ta-C is positive. At low pump energies, the thermal effect is very weak and the transient reflectivity never changes its sign, but it does not recover its unperturbed value within the investigated time window, revealing the presence of a slow carrier recombination process. As it will be proven, within the observed time interval of 20 ps, heat and carrier diffusion are negligible, thus the spatial dependence of  $N$  and  $\Delta T_L$  can be neglected.

The transient reflectivity curves at the various pump energies have been fitted allowing the simultaneous presence of carrier trapping and electron–hole bimolecular recombination, and taking into account the evolution of the lattice temperature. Including the Auger-like recombination process did not produce satisfactory fitting results, supporting the fact that the three-body mechanism takes place at much higher carrier concentrations. The following model has been used:

$$\frac{\Delta R}{R} = \alpha \left( N_1 \exp(-t/\tau_1) + \frac{N_2}{1 + \gamma_2 N_2 t} \right) + \beta (1 - \exp(-t/\tau_{ep})), \quad (5)$$

which can be interpreted in terms of a multicomponent process: (i) carrier recombination mediated by traps (first term in the rhs of equation (5)), (ii) direct electron–hole recombination



**Figure 2.** (A) Experimental transient reflectivity data (symbols) vs time delay and related fits (dotted lines) according to equation (5). Each curve corresponds to a different energy of the pump (increasing energy from top to bottom). For clarity, the curves have been offset and only 20% (every 5th point) of the experimental data are shown. (B) Time evolution of the three different contributions to the fitting model: carrier trapping (blue-solid line), bimolecular recombination (cyan-dashed line) and lattice heating (red-dotted line). The data correspond to the reflectivity curve obtained with pump energy of 1.2  $\mu\text{J}$ .

(second term in the rhs of equation (5)) and (iii) thermal effect due to lattice heating. According to equations (1) and (2), the parameter  $\alpha$  can be numerically evaluated as  $\alpha = 4(\partial n/\partial N)/(n^2 - 1) \simeq -10^{-22} \text{ cm}^3$ . On the other hand,  $\beta = 4\Delta T_0(\partial n/\partial T)/(n^2 - 1)$  is proportional to the thermo-optical coefficient  $\partial n/\partial T$  and the maximum increase of the lattice temperature  $\Delta T_0$  for a given pump fluence. Since neither  $\partial n/\partial T$  nor  $\Delta T_0$  is directly accessible with our experiment,  $\beta$  has been treated as a fitting variable. The parameters  $\tau_1$ ,  $\gamma_2$  and  $\tau_{\text{ep}}$  have been assumed to be independent from the pump energy, while  $N_1$ ,  $N_2$  (i.e. the initial photo-excited carrier densities at  $t = 0$ ) and  $\beta$  (whose fluence-dependence is implicitly given by  $\Delta T_0$ ) have been determined for each reflectivity curve. Figure 2(A) reports the experimental data and the corresponding fits according to equation (5), while figure 2(B) shows the trapping, bimolecular recombination and lattice heating contributions to the reflectivity curve measured at the intermediate pump energy of 1.2  $\mu\text{J}$ . It is also noteworthy to mention that a single recombination process (i.e. trapping or bimolecular) does not lead to acceptable fits of the curves. The fact that both recombination mechanisms must be employed can be attributed to the heterogeneous character of the ta-C film. A similar conclusion has been recently drawn by Myers *et al* [18] on the investigation of the ultrafast dynamics of nanocrystalline Si films, where different recombination mechanisms have been assigned to the nanocrystals and to the embedding amorphous matrix. In the specific case of ta-C, it has been argued that  $\text{sp}^2$  sites arrange in the form of chains dispersed inside the

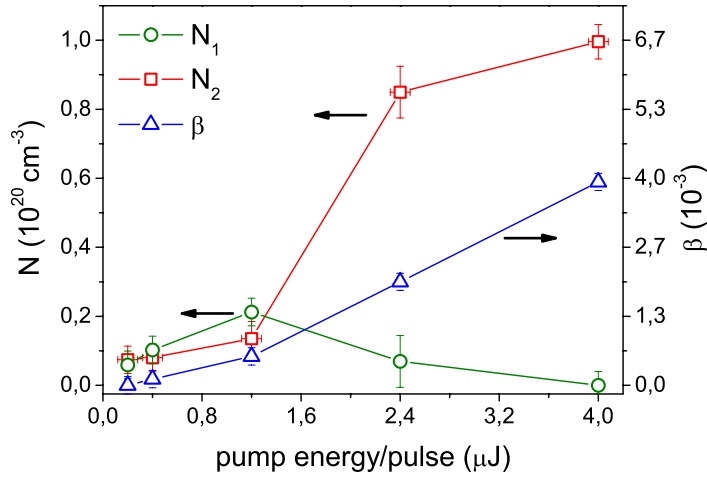


**Figure 3.** The initial photo-excited carrier densities  $N_1$  (trapping),  $N_2$  (bimolecular recombination) and the parameter  $\beta$  (proportional to the maximum lattice temperature rise  $\Delta T_0$ ) as a function of the pump energy. The data are obtained by fitting the transient reflectivity curves with equation (5).

amorphous diamond-like  $sp^3$  matrix [19]. These chains might play a role similar to nanocrystals in a-Si, as they embody localized regions of different structural phase.

The extrapolated values of the initial carrier densities  $N_1$ ,  $N_2$  and the parameter  $\beta$  are represented in figure 3 as a function of the pump energy. The density  $N_1$  of carriers recombining through traps visibly drops at high fluences, while the density  $N_2$  of carriers following the bimolecular recombination steeply increases when the pump energy is higher than  $\sim 2 \mu\text{J}$ . On the other hand, the parameter  $\beta$ , and therefore the maximum lattice temperature  $\Delta T_0$ , rises almost linearly with pump energy. The fits of the reflectivity curves allowed us to measure the electron–phonon relaxation time  $\tau_{ep} = 220 \pm 35 \text{ fs}$  from which the relaxation time  $\tau$  (i.e. the time between subsequent carrier collisions with the lattice appearing in the Drude model of the dielectric function) can be estimated. Taking  $U \sim h\nu - E_g$  as the average photo-excited carrier energy, with  $h\nu = 4.65 \text{ eV}$  being the pump photon energy and  $E_g \sim 2\text{--}3 \text{ eV}$  being the mobility gap, leads to  $U \sim 2 \text{ eV}$ . Due to electron–phonon collisions, carriers lose energy emitting phonons with average energy  $k_B T_L \sim 30 \text{ meV}$  ( $k_B$  is the Boltzmann constant and  $T_L$  is not far from room temperature with the pump fluences we used<sup>6</sup>). The rate of energy loss is simply  $dU/dt = k_B T_L/\tau$  and therefore the electron–phonon relaxation time can be written as:

$$\tau_{ep} = \frac{U}{dU/dt} = \frac{U}{k_B T_L/\tau}. \quad (6)$$

With the numerical values given above,  $\tau_{ep} \sim 70 \times \tau$ . Therefore  $\tau \sim 3 \text{ fs}$  and  $(\omega\tau)^2 \sim 50$ , justifying the approximation that led to equation (2). Knowing the value of  $\tau$  we evaluated the carrier diffusion constant from the Einstein relation:  $D_c = (k_B T)\tau/m \sim 0.2 \text{ cm}^2 \text{ s}^{-1}$  (with  $k_B T \sim 30 \text{ meV}$ ), while using the thermal properties of ta-C we quantified the heat

<sup>6</sup> The maximum lattice temperature can be estimated from the relation  $E(1-R)/(Ad) \simeq c_p \Delta T_0$ , where  $R \sim 0.3$  is the ta-C reflectivity at the pump wavelength,  $E \sim 4 \mu\text{J}$  is the highest pump energy,  $d \sim 30 \text{ nm}$  is the pump absorption length,  $A \sim 0.25 \text{ mm}^2$  is the irradiated area and  $c_p \sim 3 \text{ J cm}^{-3} \text{ K}^{-1}$  is the ta-C specific heat (see [3]). Thus  $\Delta T_0 \sim 120 \text{ K}$ .

diffusion constant  $D_h = \kappa/c_p \sim 0.03 \text{ cm}^2 \text{ s}^{-1}$  (with  $\kappa = 0.1 \text{ W cm}^{-1} \text{ K}^{-1}$  and  $c_p = 3 \text{ J cm}^{-3} \text{ K}^{-1}$ , according to [3]). Within the investigated time window  $t = 20 \text{ ps}$ , carrier (c) and heat (h) diffusion lengths are  $\lambda_{c,h} \sim \sqrt{D_{c,h}t} \leq 20 \text{ nm}$ , which is shorter than the pump absorption length, making carrier and thermal diffusion negligible.

We can now focus on the detailed analysis of the time evolution of photo-carriers: the extrapolated bimolecular recombination coefficient is  $\gamma_2 = (1.9 \pm 0.05) \times 10^{-8} \text{ cm}^3 \text{ s}^{-1}$ , being slightly larger than the value measured for amorphous [6] and nanocrystalline silicon [18], while the lifetime of carriers decaying through traps is  $\tau_1 = 550 \pm 40 \text{ fs}$ . It is interesting to notice that the term  $N_1 e^{-t/\tau_1}$  appearing in equation (5) is meaningful as long as the carrier density  $N_1$  is much smaller than the trap density  $N_t$ . Under this condition, the value of the lifetime  $\tau_1$  can be used to estimate  $N_t$ . In fact, if we assume the trap cross-section  $\sigma_t$  to be of the order of the atomic bond length squared, i.e.  $\sigma_t \sim 10^{-15} \text{ cm}^2$ , and being the carrier thermal velocity  $\langle v \rangle \sim \sqrt{3k_B T/m} \sim 10^7 \text{ cm s}^{-1}$ , we obtain  $N_t = 1/\tau_1 \sigma_t \langle v \rangle \sim 10^{20} \text{ cm}^{-3}$ . This value agrees fairly well with the density of defect states measured by electron spin resonance (ESR) in similar ta-C films [4]. We point out, however, that if the initial carrier density is close to the trap density, the exponentially decaying temporal profile fails to describe the trapping process. In fact, if  $N_1 \sim N_t$  for  $t \sim 0 \text{ ps}$ , since carriers are trapped at the same rate at which traps are filled, the relation  $N_1(t) \sim N_t(t)$  holds also for  $t > 0 \text{ ps}$ . In such a case:

$$\frac{\partial N_1}{\partial t} = -N_1/\tau_1 = -N_1 N_t \sigma_t \langle v \rangle \sim -N_1^2 \sigma_t \langle v \rangle = -\gamma_t N_1^2, \quad (7)$$

where we have defined  $\gamma_t = \sigma_t \langle v \rangle$ . Equation (7) clearly shows that the time evolution of carrier trapping is described by a bimolecular-like temporal profile when carrier and trap densities are similar. Furthermore, with the approximations given above (i.e.  $\sigma_t \sim 10^{-15} \text{ cm}^2$  and  $\langle v \rangle \sim 10^7 \text{ cm s}^{-1}$ )  $\gamma_t \sim 10^{-8} \text{ cm}^3 \text{ s}^{-1}$ , a value very close to the electron–hole recombination coefficient obtained from the fits. In view of these observations, the trends of  $N_1$  and  $N_2$  in figure 3 can be interpreted as a direct consequence of equation (7): the drop of  $N_1$  and the pronounced increase of  $N_2$  take place when the overall carrier density is roughly  $10^{20} \text{ cm}^{-3}$ , a value matching fairly well our estimate of  $N_t$ . For such a carrier density, the exponential time decay does not describe the trapping mechanism, but a bimolecular-like temporal profile arises, and consequently  $N_1$ , proportional to the exponential density decay in equation (5), drops. Accordingly, the electron–hole recombination term, proportional to  $N_2$  in equation (5), steeply increases as it also embodies the carrier trapping process. Therefore, the predominance of  $N_2$  for high pump energies does not imply that bimolecular recombination is the leading mechanism, but it is rather a consequence of the modified temporal evolution of carrier trapping. In previous studies on the ultrafast response of a-Si, the quadratic dependence of the rate equation on the optically injected carrier density  $N$  (i.e.  $\partial N/\partial t = -\gamma_2 N^2$ ) in the high excitation regime has been assigned to *nonradiative* bimolecular recombination, a particular Auger process where the deviation from the expected cubic dependence on  $N$  is attributed to spatially overlapping electron–hole pairs (see [6] and references therein). Here, we have clearly shown that for high carrier generation, the quadratic dependence is understood as a regime of carrier trapping rather than a purely nonradiative mechanism. This conclusion has also a direct consequence on the evolution of the lattice temperature: if carriers recombined mainly through nonradiative recombination, the lattice temperature would increase with a characteristic time constant  $\tau_1 = 1/N_2 \gamma_2$ , strongly depending on the carrier concentration. Our analysis instead suggests that  $\tau_{ep}$  is constant and truly represents the electron–phonon relaxation time. We finally point out that the similarity between the recombination coefficients  $\gamma_2$  of ta-C and a-Si suggests that the validity of these



observations is not specific to the carbon films, but applies more generally to amorphous and disordered semiconductors.

## 5. Conclusions

To summarize, the ultrafast carrier dynamics in ta-C has been investigated by means of femtosecond time-resolved reflectivity measurements. Photo-excited carriers follow two separate paths to recover the equilibrium condition: they can recombine (i) through localized defect states (traps) and (ii) via the bimolecular mechanism. We have shown that if the density of free carriers is comparable to the estimated density of traps, electron–hole recombination and carrier trapping assume identical time dependencies, as a consequence of the modified time evolution of the trapping process. This observation has rather general validity and sheds light on the complex ultrafast dynamics in this class of materials. It is noteworthy to emphasize that our measurements show how the time-resolved response of ta-C is qualitatively similar to that of a-Si. In view of the increasing demand for high-speed microelectronic devices and considering the outstanding mechanical and tribological properties of diamond-like materials, ta-C should be given proper consideration.

## Acknowledgments

We thank G Ghiringhelli and L Braicovich for fruitful discussions. C Manzoni and G Cerullo are gratefully acknowledged for their help with the optical experimental set-up.

## References

- [1] Drabold D A, Fedders P A and Stumm P 1994 *Phys. Rev. B* **49** 16415
- [2] Lee C H, Lambrecht W R L, Segall B, Kelires P C, Frauenheim T and Stephan U 1994 *Phys. Rev. B* **49** 11448
- [3] Morath C J, Maris H J, Cuomo J J, Pappas D L, Grill A, Patel V V, Doyle J P and Saenger K L 1994 *J. Appl. Phys.* **76** 2636
- [4] Amaratunga G A J, Robertson J, Veerasamy V, Milne W I and McKenzie D R 1995 *Diamond Relat. Mater.* **4** 637
- [5] Ronning C 2003 *Appl. Phys. A* **77** 39
- [6] Esser A, Seibert K, Kurz H, Parsons G N, Wang C, Davidson B N, Lucovsky G and Nemanich R J 1990 *Phys. Rev. B* **41** 2879
- [7] Stolk P A, Calcagnile L, Roorda S, Sinke W C, Berntsen A J M and van der Weg W F 1992 *Appl. Phys. Lett.* **60** 1688
- [8] Donay F E, Grischkowsky D and Chi C-C 1987 *Appl. Phys. Lett.* **50** 460
- [9] Cohen H H, Fritzsche H and Ocshinsky S R 1969 *Phys. Rev. Lett.* **22** 1065
- [10] Mort J and Knights J 1981 *Nature* **290** 659
- [11] Hofsäss H, Binder H, Klumpp T and Recknagel E 1993 *Diamond Relat. Mater.* **3** 137
- [12] Downer M C and Shank C V 1986 *Phys. Rev. Lett.* **56** 761
- [13] Othonos A and Christofides C 2002 *Phys. Rev. B* **66** 085206
- [14] Tanaka T, Harata A and Sawada T 1997 *J. Appl. Phys.* **82** 4033
- [15] Titantah J T and Lamoen D 2004 *Phys. Rev. B* **70** 033101
- [16] Ghosh G 1995 *Appl. Phys. Lett.* **66** 3570
- [17] Jellison G E and Burke H H 1986 *J. Appl. Phys.* **60** 841
- [18] Myers K E, Wang Q and Dexheimer S L 2001 *Phys. Rev. B* **64** 161309
- [19] Ferrari A C and Robertson J 2000 *Phys. Rev. B* **61** 14095

Copyright of New Journal of Physics is the property of IOP Publishing and its content may not be copied or emailed to multiple sites or posted to a listserv without the copyright holder's express written permission. However, users may print, download, or email articles for individual use.